Journal of Membrane Science & Technology

OPEN ACCESS Freely available online

Research Article

# NAM-PC Based Terahertz Nanosensor for Rapid Detection of Viruses and Other Molecular Entities

**Anis Rahman***

*Terahertz and Nanotechnology, Applied Research and Photonics, Harrisburg, Pennsylvania, United States*

## ABSTRACT

The pandemic caused by CoV-2 virus indicates that other unknown pandemic may occur in the future for which one must plan now. Full control of virus requires rapid diagnostics. We introduce a nanosensor system with specificity for fast detection of viruses. A novel Nanoporous Alumina Membrane Photonic Crystal (NAM-PC) is used that generates unique signature in the terahertz eigen spectrum. A terahertz eigen frequency analysis algorithm is deployed that measures the unique eigen frequencies of the NAM-PC by means of peaks in a terahertz eigen absorbance spectrum. This signature spectrum compared with the eigen absorbance spectrum of a given molecular entity (e.g., a virus), generates the signature of that virus with specificity. This principle was tested via a blank NAM-PC having 40 nm pore size and compared with that of a 25-mer Oligonucleotide Guanine (Oligo-G)'s eigen absorbance spectrum. Two prominent peaks were found in both spectra. The primary peak frequency of the Oligo-G was shifted by 0.2531 THz, while the secondary peak frequency of the same was shifted by 0.6169 THz, with respect to the blank NAM-PC. A criterion is formulated based on the combined aspects of the position of the respective peaks and the shift in the eigen frequency with respect to each other. This criterion, combined with the difference in loss factor calculated from the eigen spectra at saturation, provide unique detection technique for viruses and bio-molecular entities with high specificity. The technology may provide a go/no-go protocol for the biological samples of a patient in a few minutes.

**Keywords:** Terahertz eigen frequency; Nanosensor; Viruses; Oligonucleotide; Nanoporous substrate; Rapid detection

**Abbreviations:** NAM: Nanoporous Alumina Membrane, PC: Photonic Crystal, T-ray: Terahertz Radiation, DDE: Dendrimer Dipole Excitation, Oligo-G: Oligonucleotide Guanine, TNS3DI: Terahertz Nanoscanning Spectrometer and 3D imager, dB norm: Decibel normalized with respect to 1 MW power

## INTRODUCTION

NAM photonic crystal for nanosensing: Nanoporous Alumina Membrane Based Photonic Crystal ("NAM-PC") is a self-organized nanoporous substrate with honeycomb-like structure formed by high density arrays of uniform and parallel nanopores. As such it forms a photonic crystal with specific frequencies. NAMs are formed by electrochemical oxidation of aluminum under suitable conditions that set the growth of aluminum oxide and the localized dissolution creating the pores. In the absence of such dissolution, dense anodic alumina films are formed with limited thickness. The diameter of the nanopores can be controlled with great precision from as low as 5 nanometers to as high as a few hundred nanometers, with pore length from a few tens of nanometers to a few hundred micrometers. This route of photonic crystal fabrication is very economic as no lithographic patterning is needed. This route is also suitable for large scale production with uniformity. Figure 1 displays SEM picture of a 40 nm pore diameter NAM-PC and cleaved side view of the pores where the uniform thickness along the pore is visible. Such a porous substrate exhibits a unique signature in the terahertz regime (0.1 THz to~30 THz) which may be exploited for high sensitivity sensing with specificity [1,2]. While terahertz spectroscopic technique has been used for many investigations, however, the previous work did not consider the eigen spectrum approach.

Photonic crystal based nanosensors have been reported for virus detection without utilizing the terahertz probing. Shafiee et al., reported a photonic crystal biosensor for HIV viral load measurement [3]. Pal et al. has reported on selective virus detection in complex sample matrices with photonic crystal cavities [4]. Fathi et al. have also reported on the use of photonic crystal based biosensor for biomarker detection and Maeng et al. have reported on hydrogel based nanoporous photonic crystal for label-free rotavirus detection [5,6]. Label-free detection of Single Nucleotide Polymorphism (SNP) of short sequence and DNA hybridization

**Correspondence to:** Anis Rahman,Tetrahertz and Nanotechnology, Applied Research and Photonics, Harrisburg Pennsylvania, United States, E-mail: a.rahman@arphotonics.net

**Received:** July 06, 2021; **Accepted:** July 31, 2021; **Published:** August 7, 2021

**Citation:** Rahman A (2021) NAM-PC Based Terahertz Nanosensor for Rapid Detection of Viruses and Other Molecular Entities, 11: 247

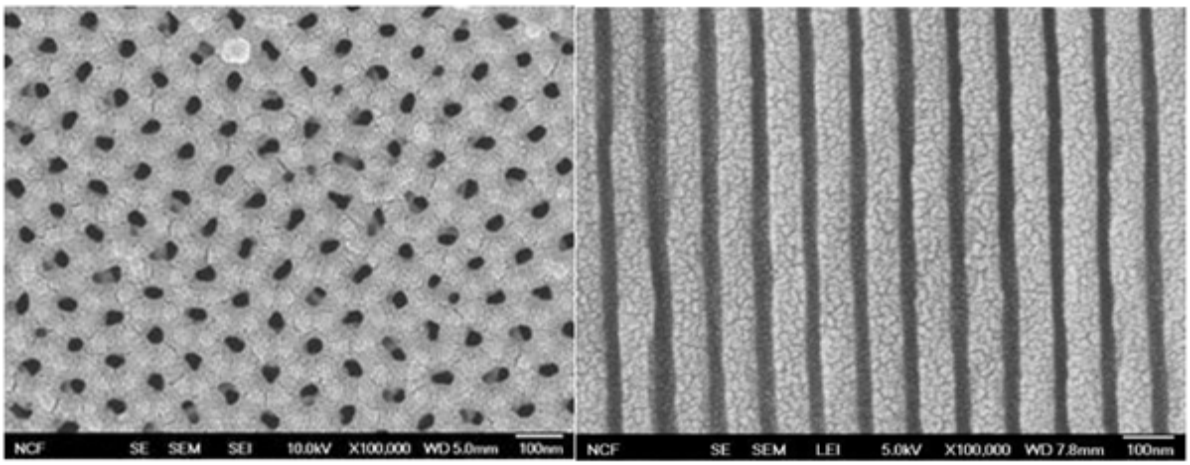


**Figure 1:** SEM image of NAM-PC. Left: Top surface, pore size 40 nm. Right: Cleaved side view showing the pores.

state *via* terahertz spectroscopy was reported by Rahman et al. [7]. In all of the above-mentioned cases the photonic crystals and label-free techniques, separately or collectively, have been used in various fashion for either the detection of viruses, biomarkers, or SNPs, etc. However, the application of a photonic crystal and the label-free technique for rapid detection of a virus or a molecular entity by terahertz eigen spectral technique has been described herein which is relatively novel.

In this paper we introduce a NAM-PC based sensing approach in conjunction with terahertz eigen spectrum for label-free rapid detection of virus and/or other molecular entities. When the terahertz eigen spectrum of a virus containing medium, such as patient saliva or blood, is compared with that of the blank substrate, specific changes in the two spectra can be quantified. Such changes occur due to the difference in mass, size and effective charge of a virus or a molecular entity. Changes may also occur due to the differences between one virus from another. The degree of these changes is measured and used as a detection technique with specificity. A probe is constructed utilizing the NAM-PC for measuring the parameters. Here, a Plexiglas plate with a small hole was used that houses the NAM-PC on one side of the hole, thus, forming a mini cuvette. This NAM-PC nanosensor is pre-characterized and the resulting spectrum is used as a reference. At this point, a small drop of saliva or blood from a patient may be applied on the mini cuvette and the terahertz eigen spectra is measured again from which the parameters are extracted. In what follows, we present some details of the eigen frequency measurement technique followed by the experimental section, results, discussion, and conclusion. Since virus sample from a real patient was not available, a sample of oligonucleotides is used as the proof of principle.

## PRINCIPLE OF TERAHERTZ SENSING

Eigen Frequency-The Eigen frequency computation algorithms offer true high-resolution frequency estimation [8,9]. The algorithm utilizes a standard procedure such as Eigen decomposition. It begins by generating an eigen decomposition from the measured data matrix using Singular Value Decomposition (SVD). The data matrices can be Forward Prediction Based (Fwd) or Forward-Backward prediction based (FB) as described below.

### Multiple Signal Classification algorithms (MSC)

After the eigen decomposition, the next step is to use the eigenvectors and eigenvalues for constructing the eigen frequency spectrum. The MSC and Eigenvector (EiV) algorithms are two of the more widely used eigen frequency calculators. These algorithms work on the principle that the noise subspace eigenvectors should be orthogonal to the signal vectors. The MSC and EiV frequency calculators are continuous reciprocal functions of frequency that have sums of products of the noise eigenvectors in the denominator. The eigen frequency peaks arise be-cause the denominator will approach zero at sinusoidal frequencies, resulting in sharp spectral peaks.

The MSC algorithm use uniform weighting. It is important that an effective signal-to-noise threshold be determined. The frequencies are identified using a two-step procedure. First, an 8193-count full-range spectrum is generated using a 16384 size Fast Fourier Transform (FFT). Then, for each peak detected, a one-dimensional minimization follows that resolves the frequency to $10^{-15}$ fractional precision. This precise estimation of frequencies is possible because the estimators are defined as continuous functions of frequency. The spectral peak count is half the signal subspace value.

The implementation of these algorithms identifies frequencies strictly from the local maxima in the output spectrum. A commercially available package, Autosignal, implements the MSC and Eigenvector procedures following the algorithm presented by Marple [8].

### Eigen spectrum formation

The MSC FB and the EiV FB algorithms are widely used primarily for extracting the sinusoidal harmonic frequencies. For estimating the frequencies of damped sinusoids, the procedures use a robust SVD eigen decomposition with appropriate weighing factors, where frequency refinement to full machine precision is automatic. It should be noted that the eigen frequency analysis procedure outlined above is applied directly on the measured time-domain interferogram as discussed below.

Eigen decomposition of signals in the absence of noise is a simple matter. For noise-free da-ta, the minimum order needed to capture any oscillatory component, harmonic or anharmonic, is twice the number of oscillatory components comprising the spectrum. In practice, however, there is usually some level of noise present in the measured data and a higher order model is needed. The additional coefficients go primarily into modeling the oscillations within the random noise. To achieve a reasonable signal-to-noise separation, it is necessary to fit a high enough order so that the

primary singular vectors (eigenvectors) span only signal space. The code utilized herein chooses an order large enough that provides sufficient signal-to-noise separation.

### Spectrum and plots

The spectrum is generated either directly or using a Fast Fourier Transform (FFT); both are built-in the computer program. The Full Range option is used that locks the 0 to 0.5 Nyquist range. The FFT options, specifies the length of the transform, while the full range option specifies the total frequency count in the output spectrum. An FFT of 16384 points produces 8193 spectral frequencies from 0 to 0.5 normalized frequencies. The estimated frequencies are refined to full machine precision regardless of the spectrum type generated.

There are two plot formats that are useful for spectral representation. The dB (Spec) plotting option uses a decibel scale. The dB norm (Spec) option plots, used in the present work, uses a normalized decibel scale, i.e., the largest peak is normalized to 0.0 dB. The dB norm option is important in that the peaks will yield an approximate ordering of power. FFT frequency estimates are based upon the local maxima in an 8193-count full-range spectrum. A $10^{-15}$ fractional error minimization is made for each of the spectral peaks. The spectral peak count is half the signal subspace value.

## EXPERIMENTAL

Details of the terahertz time-domain spectroscopy technique and the experimental setup have been described elsewhere [1,2]. In a nutshell, a Dendrimer Dipole Excitation (DDE) based continuous wave terahertz source is fabricated from a PAMAMOS dendrimer that is doped with a suitable chromophore [10]. This DDE source is utilized to design a terahertz time-domain spectrometer [1] that is used for the present work.

A blank NAM-PC nanosensor is shown in Figure 2 as mounted on a Plexiglas plate as described before. The NAM-PC is composed of an alumina membrane having an array of pores with sizes from 10 nm to 250 nm or more. The pore size on a single membrane is fixed but different substrates may have different pore sizes; this gives the specificity for a given virus. The nanosensor has an array of holes on the entire piece, as shown in Figures 1 and 3 exhibits the fiber optic circuit of the Terahertz Nanoscanning Spectrometer and 3D Imager (TNS3DI) system (from Applied Research and Photonics, Inc., Harrisburg, PA) that measures the terahertz intensity after the incident T-ray being interacted with the NAM-PC, both in reflection and in transmission. The fiber optic circuit is comprised of a multimode optical fiber, a plurality of beam steering lenses, a plurality of beam focusing mechanism, a mechanism for interacting the T-ray beam with specimens, and a mechanism for collecting the post-interaction T-ray photons in both re-flection and in transmission, thus forming the nanosensing element for detection. The nano-sensing element thus formed, is capable of sensing the presence or absence of a virus species after calibration, whose size parameter may range from a few nanometers up to more than a micrometer.

The arrow in Figure 3 indicates the sample mounting mechanism. Figure 4a and Figure 4b exhibits a close-up of the NAM-PC as mounted on the TNS3DI. All NAM-PC nanosensors affixed on the Plexiglas plate were mounted on the TNS3DI one at a time. Several time-domain interferograms were acquired for each NAM-PC *via* the pump-probe technique implemented on the TNS3DI [1]; an average of the interferograms was used to compute the eigen frequency absorbance spectrum. All measurements were carried out by the TNS3DI's front-end software.

After the reference spectrum corresponding to a blank NAM-PC was established, the effectiveness of the NAM-PC nanosensor technique for detection ability was tested by dropping 20 µL of a 25-mer Oligonucleotide Guanine (Oligo-G) solution (2 mm) in Tris-EDTA (TE) buffer. This 25-mer single stranded DNA sequence has a molecular weight of 8.168 kDa and calculated mass in 20 µL solution is 326.727 µg [10]. In order to allow the interaction of the Oligo-G with the probing T-ray, first the TE buffer (solvent) was allowed to dry. Drying kinetics was monitored to determine the sample stability as a function of time. Kinetics data were collected until such time so that all time-dependent changes could be monitored until saturation. When the kinetics reached saturation indicating the completion of drying, the pump-probe technique was used to capture the time-domain interferograms corresponding to

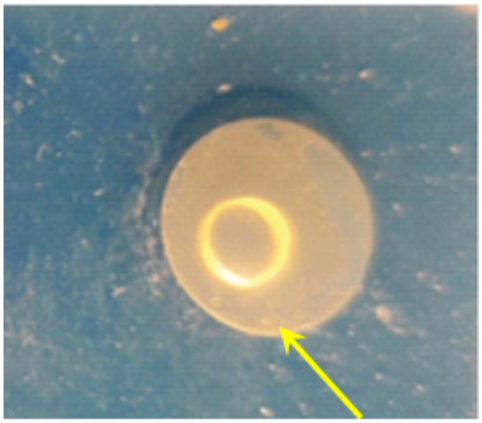

**Figure 2:** A NAM-PC nanosensor mounted on a plexiglas plate over a hole. The entire NAM has a uniform array of holes of 40 nm diameter (indicated by the arrow).

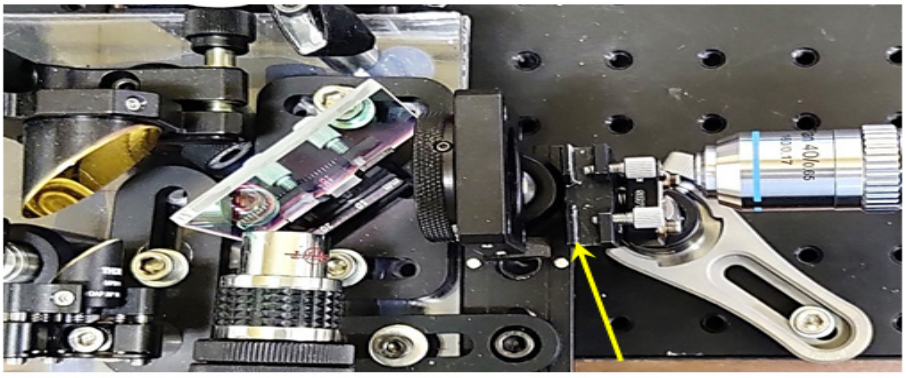

**Figure 3:** Optical circuit of the Nano scanner. The arrow indicates the sample mounting arrangement.

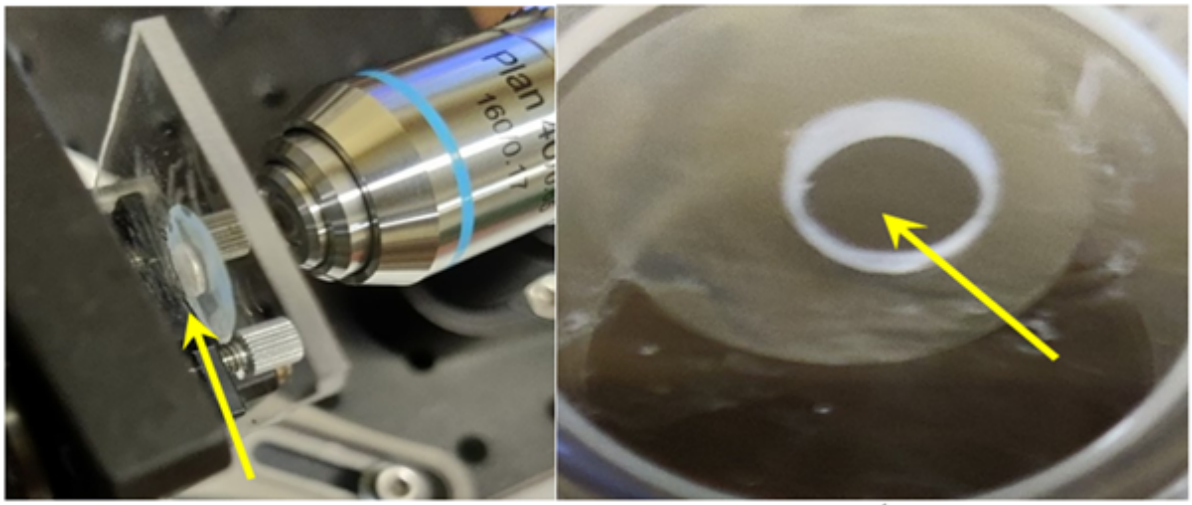


**Figure 4:** A): Close up of the blank NAM-PC mounted on the nanoscanner B): 20 µL Oligo-G 2 mm solution in TE buffer applied in the plexiglas well on to the NAM nanosensor.

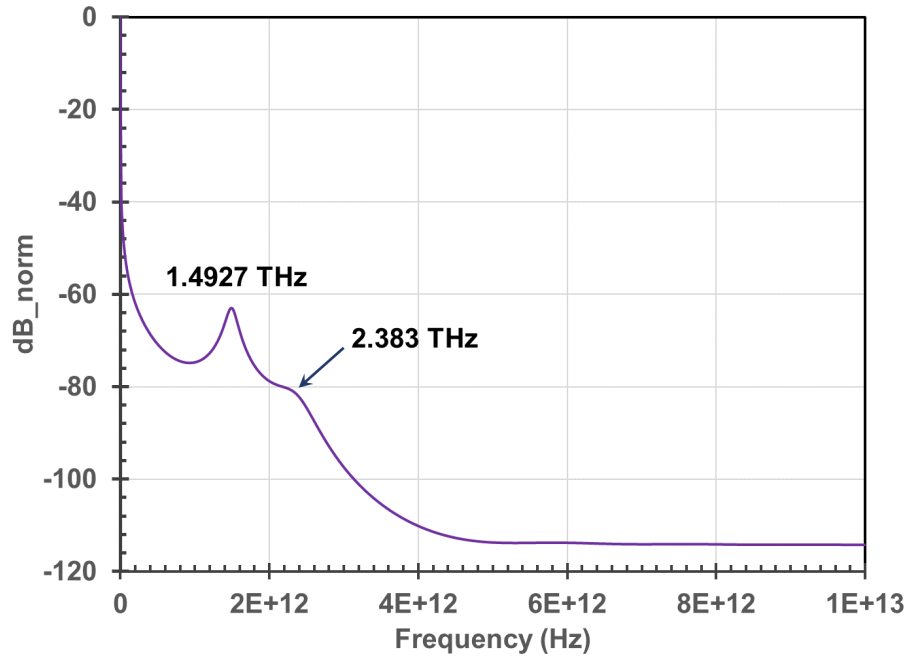


**Figure 5:** The eigen frequency absorbance spectrum indicates a major peak at 1.4927 THz for the blank NAM-PC nanosensor.

the dry Oligo-G on the NAM. Several interferograms were collected; an average of these interferograms was used for the spectral analysis via aforementioned MSC eigen analysis procedure. The results are presented below.

## RESULTS

### Eigen frequency absorbance spectrum

Figure 5 exhibits a terahertz eigen absorbance spectrum of a blank NAM-PC nanosensor obtained from the average of 5 pump-probe interferograms *via* the MSC algorithm described before. The eigen spectrum indicates a major peak at 1.4927 THz and a minor peak at 2.3831 THz for the blank NAM-PC.

Figure 6 exhibits the drying kinetics of the 20 µL Oligo-G solution (2 mm) in TE buffer applied to the Plexiglas well on top of the blank NAM-PC. The TE buffer has completely evaporated at around 1500 s, leaving the Oligo-G on the NAM-PC nanosensor. At this point the time domain pump-probe interferograms were acquired for the Oligo-G and an average interferogram was used for eigen absorbance spectrum computation, as depicted in Figure 7. A sharp peak (major peak) is seen at 1.2396 THz and a minor peak is observed at 3.0 THz.

Figure 8 displays a combined plot of the eigen absorbance spectra of blank NAM-PC *vs.* G-Oligo. It is seen that both spectra saturate at ~6 THz; the blank NAM-PC is lossier than the G-Oligo. The loss factor difference at saturation is~6.73 dB; this is used as an identifying parameter (Δ3) along with the frequency shifts in the major and minor peaks.

Figure 9 exhibits a close up of Figure 8. The shifts of the peak frequencies of G-Oligo compared to the blank NAM-PC are quantified. The primary shift (Δ1), computed from the major peaks is 0.2531 THz while the minor shift, (Δ2), computed from the minor peaks is 0.6169 THz.

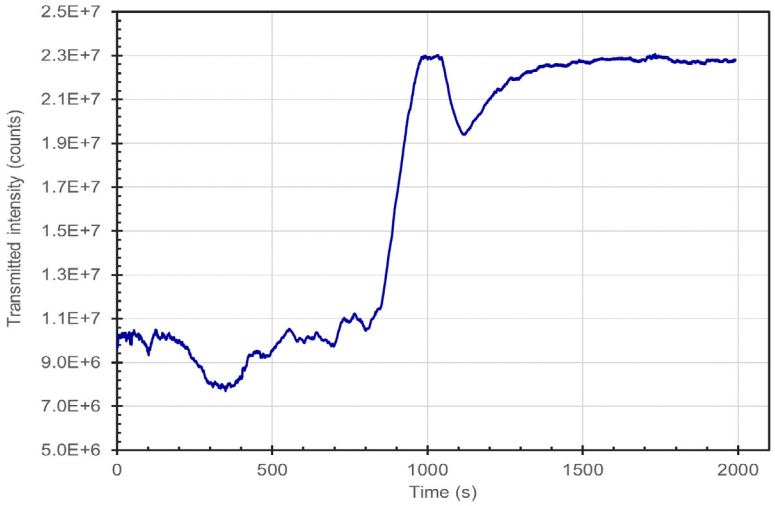


**Figure 6**: Drying kinetics of 2 mm Oligo-G solution in TE buffer applied to the NAM-PC nanosensor.

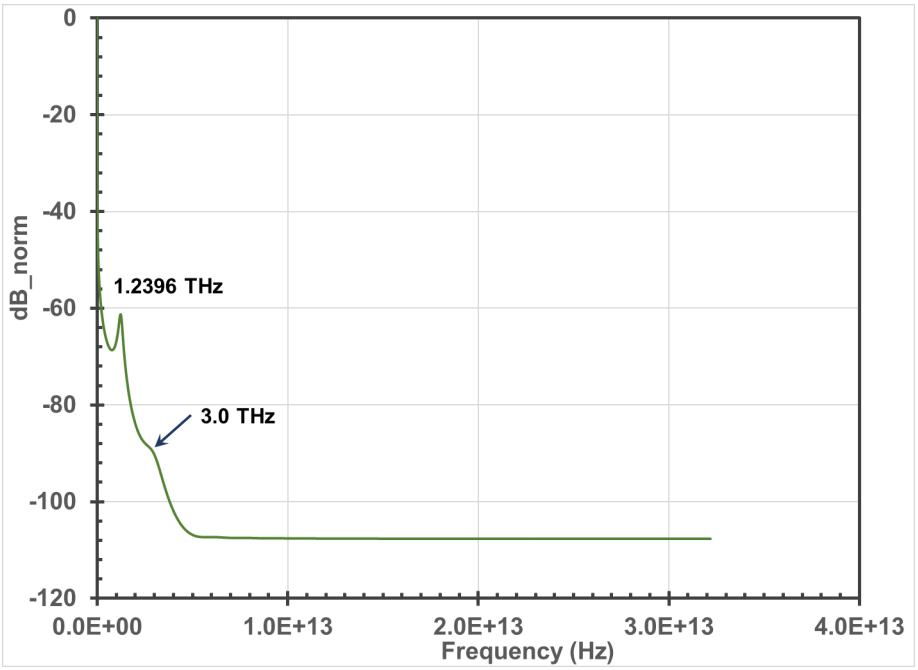


**Figure 7**: Eigen spectra of Oligo-G exhibiting a prominent peak at 1.2396 THz. This is compared with the blank NAM-PC.

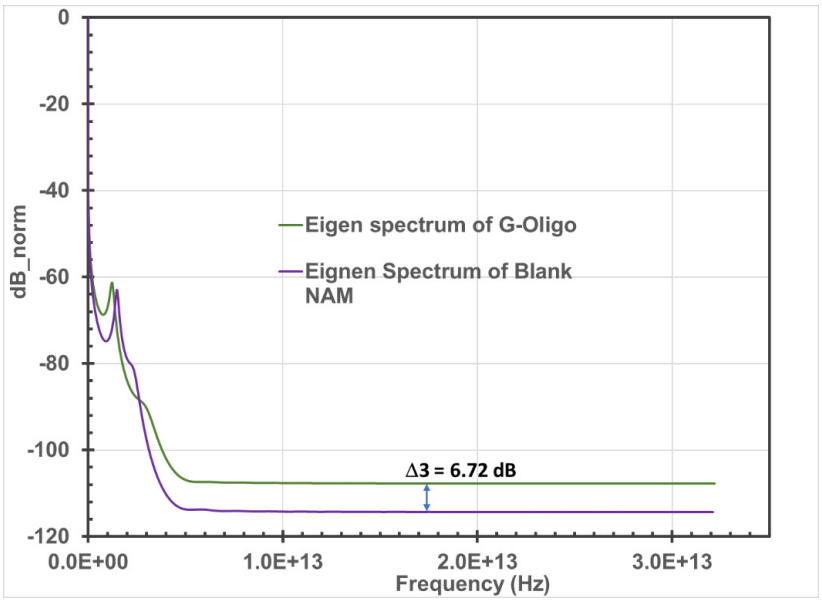


**Figure 8**: Combined plot of the eigen spectrum of blank NAM-PC *vs.* Oligo-G. Spectra saturates at ~6 THz showing the blank NAM is lossier than the Oligo-G. The loss factor difference at saturation is ~6.73 dB; this may be used as an identifying parameter.

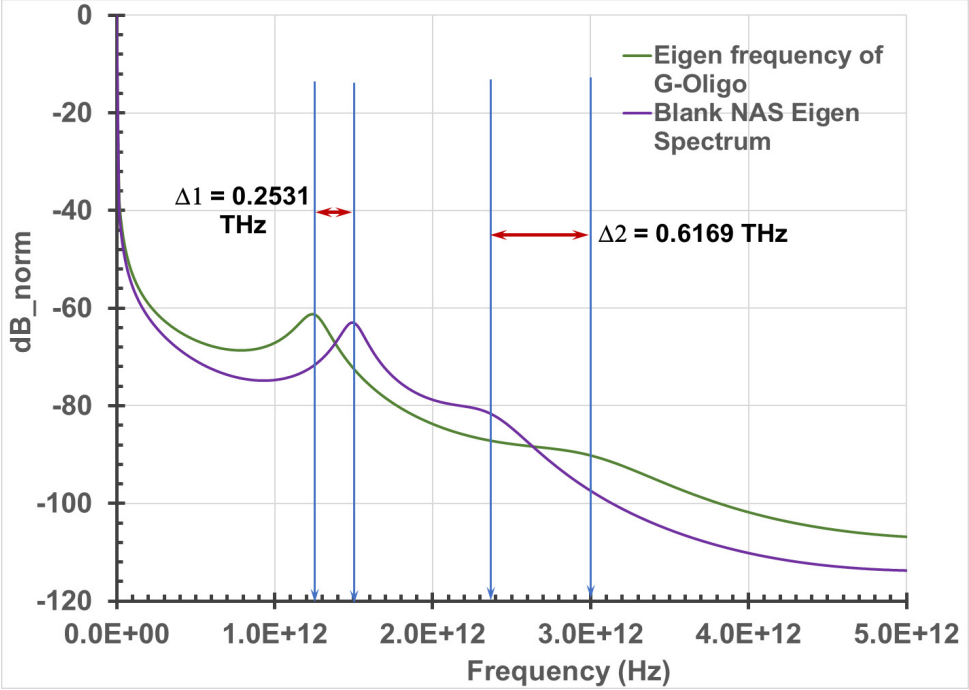


**Figure 9**: Close up of Figure 8. The shift (Δ) of peak frequency of the Oligo-G compared to the blank NAM-PC are quantified.

## DISCUSSION

While the ultimate goal is to utilize the technique discussed herein for detection of viruses and bacteria, the present data acquired from the Oligo-G solution was used only as a proof of principle. Nonetheless, the data presented herein do provide evidence for detectability of small quantity molecular species when calibrated for the shifts in the eigen frequency corresponding to a given molecular entity. As seen in Figure 9, the secondary eigen frequency peaks are wide, as such the peak determination involves some uncertainty. However, the primary eigen frequency peaks are sharp, allowing accurate determination of the peak values. The tasks ahead will involve working out an analytical model for predicting the eigen frequency of a given species and refine that in terms of the measured values. Real virus samples also will be tested to confirm the technique for rapid diagnostic purposes.

The three eigen parameters (Δ1, Δ2, and Δ3) as defined, correspond to mass parameter Δ1 obtained from the primary peak's shift of the eigen absorbance spectra; the size parameter Δ2 obtained from the shift of the secondary peak of the eigen absorbance spectra; and the effective charge parameter Δ3 which is the value of loss factor obtained from the difference of the spectra at saturation. The eigen parameters Δ1 and Δ2 have units of Hz, and the loss parameter Δ3 has the unit of dB. Since the mathematical expressions for the computation algorithm utilized in this work are well established [8,9], a review of the mathematical equations was avoided for the sake of focusing on the conceptual discussion of the technique. The measurement technique has been emphasized for the detection application of the algorithm.

While the data on the Oligo-G of the present investigation provides a proof of concept, however, the real virus sample will be investigated as the next step. Another issue is after drying a trace quantity of salts in TE buffer is present on the NAM-PC. This may seem to be a contributor of quantitative discrepancy; however, for a fixed concentration (2 mm) and fixed amount of solution (20 μL), the very small (trace) quantity of residue from the TE buffer will always be the same. This trace residue will be a part of the reference; hence, will not be a source of discrepancy. The NAM-PC and TE buffer combination, thus, provides a valid reference for the Oligo-G of the present investigation. Further investigation will be conducted for calibration with respect to a given virus or a molecular entity. The NAM-PC nanosensor interrogated by the T-ray provides a route to selective detection.

## CONCLUSION

A NAM-PC nanosensor system for rapid detection of viruses and molecular entities has been designed and tested where terahertz eigen absorbance spectra are utilized for identification of a specific molecular species. A NAM-PC with varying pore sizes is used for specificity for a given molecular entity; and a T-ray beam is used for interrogation of both the NAM-PC and the molecular entity or a given virus. To our knowledge, this is the first effort where an eigen frequency approach has been utilized for the detection of molecular entities. The three parameters (Δ1, Δ2, and Δ3) as defined in the text, aid in a good specificity for a given molecular entity such as a virus or a bacterium. The NAM-PC nanosensor system comprised of a NAM-PC, a terahertz spectrometer, a fiber optic circuit for delivering the T-ray beam to the specimen, modules for simultaneous measurement of transmitted and reflected signals, and a spectral analysis module for generating the specimen signature. The principle was tested with an oligonucleotide, the Oligo-G. It was found that there are sharp eigen frequency peaks in the eigen absorbance spectra of both the blank NAM and the Oligo-G with a shift of 0.2531 THz with respect each other. There is also a secondary peak in both spectra that are shifted by 0.6169 THz with respect to each other. This principle is equally applicable to any molecular species including the viruses.

## ACKNOWLEDGMENT

The author wishes to acknowledge partial funding provided by the Anthropocene Institute, 2450 Hannover St., Suite 100, Palo Alto CA, 94304.

## REFERENCES

1. Rahman A. Dendrimer based terahertz time-domain spectroscopy and applications in molecular characterization. J Mol Str. 2011;1006(1-3):59-65.
2. Rahman A, Rahman AK, Tomalia DA. Engineering dendrimers to produce dendrimer dipole excitation based terahertz radiation sources suitable for spectrometry, molecular and biomedical imaging. Nanoscale horiz. 2017;2(3):127-134.
3. Shafiee H, Lidstone EA, Jahangir M, Inci F, Hanhauser E, Henrich TJ, et al. Nanostructured optical photonic crystal biosensor for HIV viral load measurement. Sci Rep. 2014;4(1):1-7.
4. Pal S, Yadav AR, Lifson MA, Baker JE, Fauchet PM, Miller BL. Selective virus detection in complex sample matrices with photonic crystal optical cavities. Biosens and Bioelectro. 2013;44:229-234.
5. Fathi F, Rashidi MR, Pakchin PS, Ahmadi KS, Nikniazi A. Photonic crystal based biosensors: Emerging inverse opals for biomarker detection. Tal. 2020; 121615.
6. Maeng B, Park Y, Park J. Direct label-free detection of rotavirus using a hydrogel based nanoporous photonic crystal. RSC adv. 2016;6(9):7384-7390.
7. Rahman A, Ara G, Rahman AK, Stanley B. Label-free detection of single nucleotide polymorphism and DNA hybridization by terahertz spectrometry. Int Med rev. 2016.
8. Marple Jr SL, Carey WM. Digital spectral analysis with applications. 1987, pp.361-378.
9. Steven MK. Modern spectral estimation. Prentice Hall. 1988;13: 429-434.
10. DNA Calculator Tool.